SQUIDs: Macroscopic Quantum Coherence, Sensing, and Computation

Agha Tasheer Syedi[1]

cs.aghasyedi@gmail.com
[1]School of Quantum Technology, DIAT, Pune, India

February 14, 2026

Abstract

Superconducting Quantum Interference Devices (SQUIDs) represent the pinnacle of macroscopic quantum phenomena, serving as the critical interface between classical electronics and the quantum domain. This paper provides a comprehensive review of the theoretical foundations, operational architectures, and fabrication methodologies of SQUIDs. Beginning with the historical development of superconductivity and the Ginzburg–Landau framework, we derive the governing principles of the Josephson effect and magnetic flux quantization that enable the transduction of femtotesla-scale magnetic fields into readable voltage signals. We analyze the distinct operating modes of DC and RF SQUIDs, evaluating their current-phase relations, transfer functions, and fundamental noise limits—ranging from thermal Johnson noise to the Heisenberg uncertainty principle. The review further examines the materials science required for device realization, contrasting low-T_c Niobium trilayer processes with High-T_c YBCO grain boundary junctions. Crucially, this work details the paradigm shift of the SQUID from a passive magnetometer to an active element in quantum information processing. We discuss the role of SQUIDs in the architecture of superconducting qubits (Flux, Phase, and Transmon), quantum-limited parametric amplification (JPA), and hybrid quantum systems. Finally, we explore the research frontiers of topological Josephson junctions hosting Majorana zero modes and the utilization of SQUIDs in the search for axion dark matter, outlining the future trajectory of quantum sensing and computation.

Keywords: Superconductivity, SQUID (Superconducting Quantum Interference Device), Josephson Effect, Flux Quantization, Quantum Computing, Transmon Qubit, Quantum Metrology, Parametric Amplification, Topological Superconductors, Dark Matter Detection.

FOUNDATIONS OF SUPERCONDUCTIVITY

1 HISTORICAL DEVELOPMENT

The path to understanding Superconducting Quantum Interference Devices (SQUIDs) begins with the fundamental breakdown of classical resistivity and the emergence of macroscopic quantum phenomena in materials.

1.1 Discovery of Superconductivity

Superconductivity was first observed in 1911 by Heike Kamerlingh Onnes at Leiden University. While investigating the electrical resistance of mercury at cryogenic temperatures, Onnes observed a phenomenon that defied the classical Drude model of conduction. As the temperature of the mercury was lowered below a critical threshold ($T_c = 4.2$ K), the DC electrical resistance did not merely approach a small residual value due to impurities; rather, it vanished abruptly.

This state of perfect conductivity implies that a current loop initiated in a superconductor can persist indefinitely without attenuation, a property crucial for the persistent current modes utilized in SQUIDs.

1.2 Meissner Effect

For over two decades, superconductivity was viewed simply as ideal conductivity ($\rho = 0$). However, in 1933, Walther Meissner and Robert Ochsenfeld discovered that a superconductor is more than a perfect conductor; it is a perfect diamagnet.

When a material transitions into the superconducting state in the presence of a weak external magnetic field, it actively expels the magnetic flux from its interior. This expulsion is known as the Meissner Effect. Mathematically, inside the bulk of the superconductor:

$$\vec{B} = 0 \tag{1}$$

This implies a magnetic susceptibility of $\chi = -1$. This distinction is vital: a perfect conductor (following Lenz's law) would trap existing magnetic flux if cooled in a field, whereas a superconductor expels it, proving that the superconducting state is a distinct thermodynamic phase, independent of the history of cooling.

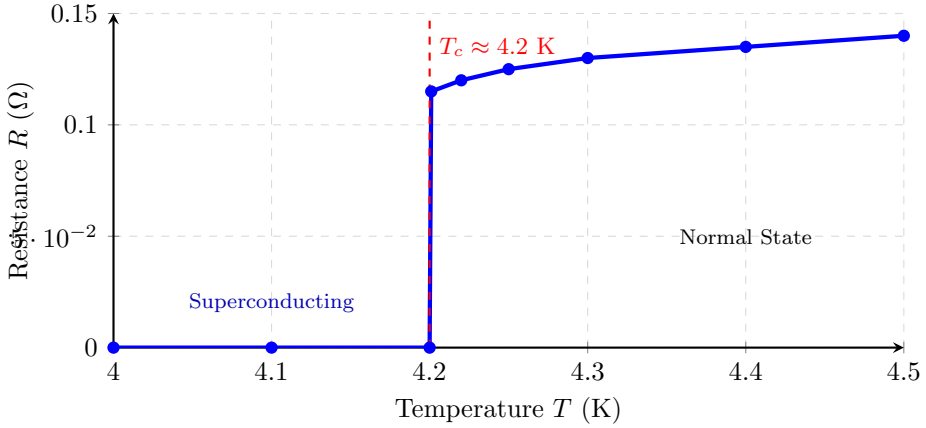

Figure 1: The historical measurement of resistance versus temperature for mercury, illustrating the abrupt phase transition at the critical temperature T_c.

1.3 Type I vs Type II Superconductors

Superconductors are categorized based on their response to increasing magnetic fields.

1. **Type I Superconductors:** Typically elemental metals (Pb, Hg, Sn). They exhibit perfect Meissner effect (complete flux expulsion) up to a critical magnetic field H_c. Above H_c, superconductivity is destroyed abruptly, and the material reverts to the normal state.

2. **Type II Superconductors:** Typically alloys and complex compounds (NbTi, YBCO). These materials possess two critical fields, H_{c1} and H_{c2}.

    - Below H_{c1}, the material is in the Meissner state.
    - Between H_{c1} and H_{c2}, the material enters the *mixed state* (or Abrikosov state). Here, magnetic flux penetrates the material in quantized filaments known as vortices. The core of each vortex is normal (non-superconducting), surrounded by circulating supercurrents.

SQUIDs generally utilize Type I materials or Type II materials operating in low-field regimes to maintain rigorous phase coherence without the noise introduced by vortex motion.

2 THEORETICAL FRAMEWORK

To engineer quantum devices, we require a mathematical description of how electromagnetic fields interact with the superconducting condensate.

2.1 London Equations

In 1935, Fritz and Heinz London proposed a phenomenological theory to describe the electrodynamics of the superconducting state. They postulated that the supercurrent density $\vec{J_s}$ is governed by the local magnetic vector potential $\vec{A}$.

The second London equation explains the Meissner effect:

$$\nabla \times \vec{J}_s = -\frac{n_s e^2}{m}\vec{B} \tag{2}$$

where n_s is the number density of superconducting carriers. Combining this with Maxwell's equations leads to the prediction that magnetic fields decay exponentially inside a superconductor:

$$B(x) = B_0 e^{-x/\lambda_L} \tag{3}$$

Here, λ_L is the **London Penetration Depth**, a characteristic length scale (typically 50-500 nm). This defines the "skin" of the SQUID loop where supercurrents actually flow.

2.2 Ginzburg–Landau Theory

While the London theory describes electrodynamics, the Ginzburg-Landau (GL) theory (1950) provides a thermodynamic framework. It introduces a complex order parameter $\psi(\vec{r})$, where $|\psi(\vec{r})|^2 = n_s(\vec{r})$, representing the local density of superconducting electrons.

GL theory introduces a second characteristic length scale, the **Coherence Length** (ξ). This represents the distance over which the superconducting order parameter ψ can vary without an excessive energy penalty. The ratio of the two length scales defines the Ginzburg-Landau parameter:

$$\kappa = \frac{\lambda_L}{\xi} \tag{4}$$

- If $\kappa < 1/\sqrt{2}$, the material is Type I (surface energy is positive).
- If $\kappa > 1/\sqrt{2}$, the material is Type II (surface energy is negative, favoring flux penetration).

2.3 BCS Theory and Cooper Pair Formation

In 1957, Bardeen, Cooper, and Schrieffer (BCS) provided the microscopic quantum theory. They showed that in a superconductor, electrons (fermions) couple together to form bound pairs known as **Cooper Pairs**.

- **Mechanism:** An electron moving through the crystal lattice attracts positive ions, creating a local deformation (phonon). A second electron is attracted to this deformation. This effective electron-electron attraction overcomes the Coulomb repulsion.
- **Bosonic Nature:** A Cooper pair has integer spin (spin 0 for conventional superconductors). Consequently, these pairs can condense into a single macroscopic quantum ground state.
- **Energy Gap (2Δ):** The formation of pairs lowers the system's energy. Breaking a pair requires a minimum energy input, protecting the current from scattering (resistance) as long as thermal or kinetic energy is below this gap.

3 QUANTUM PHASE AND FLUX QUANTIZATION

This section establishes the direct operating principle of SQUIDs: the manipulation of the macroscopic quantum phase.

3.1 Macroscopic Wavefunction

Because Cooper pairs act as bosons and condense into the same ground state, the entire ensemble of 10^{23} electrons can be described by a single macroscopic wavefunction:

$$\Psi(\vec{r},t) = \sqrt{n_s(\vec{r})}e^{i\theta(\vec{r},t)} \tag{5}$$

where n_s is the density of Cooper pairs and θ is the macroscopic quantum phase. In a SQUID, the variable of interest is usually the phase difference $\Delta\theta$ rather than the density.

3.2 Phase Coherence

In a normal metal, electron phases are random. In a superconductor, phase coherence extends over macroscopic distances. This "stiffness" of the wavefunction means that varying the phase θ requires energy and generates supercurrent.

The quantum mechanical current density in the presence of a magnetic field (vector potential $\vec{A}$) is given by:

$$\vec{J_s} = \frac{n_s q\hbar}{m}\left(\nabla\theta - \frac{q}{\hbar}\vec{A}\right) \tag{6}$$

where $q = -2e$ (charge of a Cooper pair). This equation links the mechanical momentum (current) directly to the electromagnetic momentum ($\vec{A}$) and the gradient of the quantum phase.

3.3 Magnetic Flux Quantization

Consider a superconducting ring (the basic geometry of a SQUID). The wavefunction Ψ must be single-valued. This means that if we traverse a closed path Γ around the ring, the phase θ must change by an integer multiple of 2π:

$$\oint_\Gamma \nabla\theta \cdot d\vec{l} = 2\pi n, \quad n \in \mathbb{Z} \tag{7}$$

Using the relation between current, phase, and vector potential derived in Section 1.3.2, and integrating around a loop deep inside the superconductor where $\vec{J_s} \approx 0$, we find that the magnetic flux Φ enclosed by the ring is quantized.

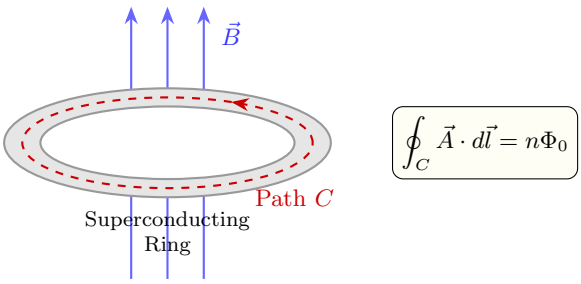

Figure 2: Flux quantization in a superconducting ring. The magnetic flux Φ trapped inside the ring is restricted to integer multiples of the flux quantum $\Phi_0 \approx 2.07 \times 10^{-15}$ Wb.

The unit of quantization is the **Magnetic Flux Quantum**:

$$\Phi_0 = \frac{h}{2e} \approx 2.0678 \times 10^{-15} \text{ Wb} \tag{8}$$

This extremely small value is the fundamental "bit" of information in superconducting electronics. A SQUID does not merely measure flux; it acts as a flux-to-voltage transducer capable of resolving fractions of Φ_0, allowing for sensitivity limits approaching the quantum limit.

JOSEPHSON EFFECT: THE CORE OF SQUIDS

4 INTRODUCTION

In the previous part, we established that a superconductor is described by a single macroscopic wavefunction, $\Psi = \sqrt{n_s}e^{i\theta}$. The Superconducting Quantum Interference Device (SQUID) relies on the ability to manipulate the phase θ not just within a bulk material, but across a discontinuity.

This discontinuity is known as a *weak link* or a *Josephson Junction*. It essentially acts as a valve for the supercurrent, where the flow is governed strictly by the quantum mechanical phase difference across the barrier. This part details the physics of this tunneling phenomenon, which forms the active element of all SQUID sensors.

5 JOSEPHSON JUNCTION FUNDAMENTALS

5.1 Tunneling of Cooper Pairs

Classically, if two superconductors are separated by an insulating barrier (typically an oxide layer of $10 - 20$ Å), no current should flow unless the voltage exceeds the breakdown threshold. However, in the quantum regime, wavefunctions do not terminate abruptly at a wall; they decay exponentially.

In a Josephson Junction, the insulating barrier is sufficiently thin that the macroscopic wavefunctions of the two superconducting electrodes (Ψ_1 and Ψ_2) overlap within the barrier region.

Unlike single-electron tunneling (Giaever tunneling), which is dissipative and requires breaking a Cooper pair (costing energy Δ), **Josephson tunneling** involves the transfer of Cooper pairs. Since Cooper pairs are bosons residing in the ground state, they can tunnel from one side to the other without energy loss, provided the phase relationship allows it. This maintains phase coherence across the entire device, effectively making the two superconductors a single quantum system despite the physical separation.

5.2 DC Josephson Effect

The most striking consequence of this overlap is the DC Josephson Effect. It states that a supercurrent can flow through the insulating barrier *in the absence of any applied voltage.*

If we connect a current source to the junction and slowly increase the current from zero, the junction will remain at $V = 0$. The current is carried entirely by the tunneling Cooper pairs. This supercurrent is not driven by an electric field (voltage), but rather by the **phase difference** $\phi = \theta_2 - \theta_1$ between the two superconducting electrodes. As the external circuit pushes more current, the phase difference ϕ adjusts automatically to accommodate this flow, up to a critical maximum value.

5.3 AC Josephson Effect

If the applied current exceeds the critical current (I_c) of the junction, the coupling energy can no longer sustain the phase lock. The junction switches to a resistive state, and a finite voltage V appears across it.

Remarkably, applying a constant DC voltage V_{DC} across the junction causes the phase difference ϕ to evolve linearly with time. Because the current depends on the sine of this phase (as detailed in Section 2.2), the result is an alternating current (AC) oscillating at a frequency proportional to the applied voltage.

This effect converts a voltage (a difficult quantity to measure precisely at low levels) into a frequency (which can be measured with extreme precision).

6 JOSEPHSON EQUATIONS

In 1962, Brian Josephson derived two fundamental equations that describe the dynamics of the junction. These are the constitutive relations for the SQUID.

6.1 Current–Phase Relation (First Josephson Equation)

The first equation relates the supercurrent I_s flowing through the junction to the phase difference ϕ across it:

$$I_s = I_c \sin(\phi) \tag{9}$$

Where:

- I_s is the supercurrent.
- I_c is the **Critical Current**, the maximum supercurrent the junction can support before developing a voltage. I_c depends on the thickness and material of the barrier and the temperature.
- $\phi = \theta_2 - \theta_1$ is the gauge-invariant phase difference.

Physical Intuition: This relation implies nonlinearity. Unlike a resistor ($I = V/R$) or inductor ($V = LdI/dt$), the Josephson junction behaves as a non-linear inductor where the "stiffness" of the coupling depends on how "twisted" the phase is. The energy stored in the junction is minimized when $\phi = 0$, and current flows to restore this equilibrium.

6.2 Voltage–Frequency Relation (Second Josephson Equation)

The second equation describes how the phase difference evolves in the presence of a voltage V:

$$\frac{d\phi}{dt} = \frac{2e}{\hbar} V \tag{10}$$

Where $\hbar$ is the reduced Planck constant and e is the elementary charge. This equation can be rewritten using the magnetic flux quantum $\Phi_0 = h/2e$:

$$\frac{d\phi}{dt} = \frac{2\pi}{\Phi_0} V \tag{11}$$

Physical Intuition: This states that the rate of change of the quantum phase is directly proportional to the potential energy difference (voltage) across the junction.

- If $V = 0$ (DC Effect), then $d\phi/dt = 0$. The phase is constant, and a constant DC supercurrent flows ($I = I_c \sin(\text{const})$).
- If $V = V_{DC}$ (AC Effect), then $\phi(t) = (2\pi V_{DC}/\Phi_0)t + \phi_0$. Substituting this into the first equation yields $I(t) = I_c \sin(\omega_J t)$, where the Josephson frequency is $f_J = V/\Phi_0 \approx 483.6$ GHz/mV.

7 JUNCTION TYPES

While the theoretical description applies generally, the physical realization of the "weak link" determines the device's performance, hysteresis, and capacitance.

7.1 SIS Junctions (Superconductor-Insulator-Superconductor)

The SIS junction is the classic "sandwich" structure, typically made of Niobium-Aluminum Oxide-Niobium (Nb-AlOx-Nb).

- **Structure:** Two superconducting films separated by a thin oxide layer.
- **Characteristics:** High resistance and high capacitance.

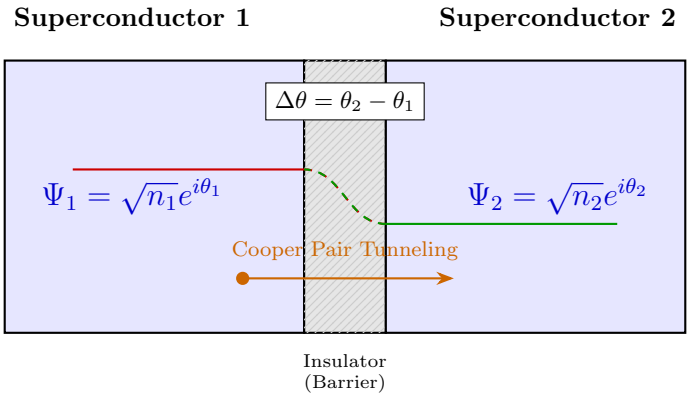

Figure 3: Schematic of Cooper pair tunneling in a Josephson junction. The macroscopic wavefunctions Ψ_1 and Ψ_2 extend into the thin insulating barrier, creating an overlap that allows a supercurrent to flow, governed by the phase difference $\Delta\theta$.

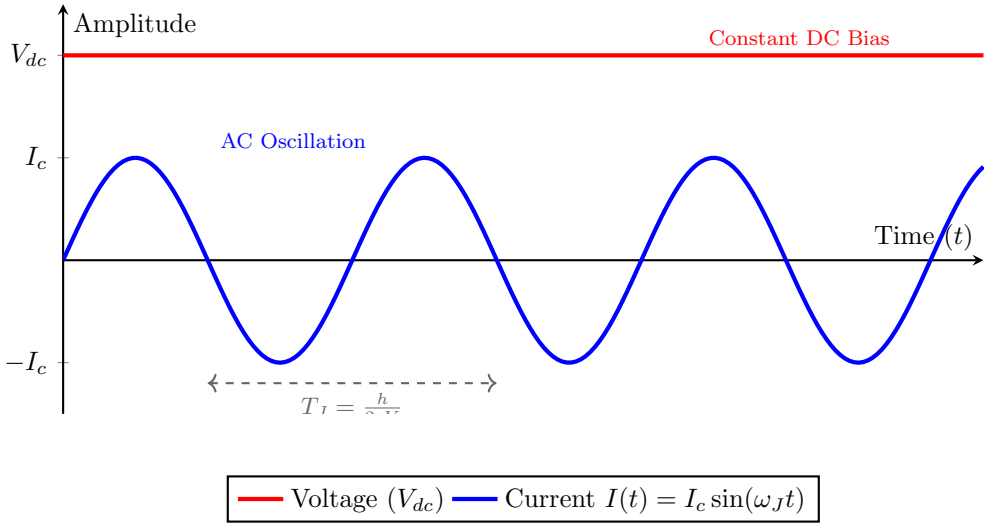

Figure 4: The AC Josephson effect: A constant DC voltage V_{dc} creates a phase difference that increases linearly with time, resulting in a sinusoidal supercurrent oscillation at the frequency $f_J = 2eV/h$.

- **Implication:** The high capacitance leads to hysteretic I-V curves (the voltage does not return to zero at the same current it left zero). While excellent for digital logic (RSFQ), hysteresis is undesirable for SQUIDs, which require a smooth, single-valued response. Therefore, SIS junctions in SQUIDs are often "shunted" with an external resistor to dampen the hysteresis.

7.2 SNS Junctions (Superconductor-Normal-Superconductor)

In an SNS junction, the barrier is a normal metal (like Gold or Copper) rather than an insulator.

- **Structure:** The superconductor is interrupted by a short bridge of normal metal.
- **Mechanism:** Superconductivity is induced in the normal metal via the *Proximity Effect*. Cooper pairs diffuse into the normal metal, retaining coherence over a short distance.
- **Characteristics:** inherently low resistance and negligible capacitance.
- **Implication:** These junctions are naturally "overdamped" (non-hysteretic). This makes them ideal for SQUIDs as they provide a stable, single-valued voltage response to magnetic flux without needing external shunt resistors.

7.3 Grain Boundary Junctions

These are primarily relevant to High-Temperature Superconductors (HTS) like YBCO (Yttrium Barium Copper Oxide).

- **Structure:** Creating oxide barriers in complex ceramics like YBCO is extremely difficult. Instead, two crystals of the superconductor are grown such that their crystal lattices are misaligned by a specific angle (e.g., 24°).
- **Mechanism:** The interface where the mismatched lattices meet acts as a natural weak link, restricting current flow.
- **Implication:** While simpler to fabricate than multilayer HTS structures, grain boundaries are

often "noisy" due to the random motion of flux vortices trapped in the boundary. However, they are essential for SQUIDs operating at liquid nitrogen temperatures (77 K).

SQUID ARCHITECTURES AND OPERATING PRINCIPLES

8 INTRODUCTION

Having established the principles of flux quantization and the Josephson effect, we now combine these phenomena to construct the Superconducting Quantum Interference Device (SQUID). The SQUID is essentially a flux-to-voltage transducer that exploits the quantum interference of wavefunctions to detect magnetic flux changes with sensitivity approaching the quantum limit. This part details the operational mechanics of the two primary SQUID architectures: the DC SQUID and the RF SQUID.

9 BASIC CONCEPT OF SQUID

9.1 Interference of Superconducting Wavefunctions

The operation of a SQUID is directly analogous to the classic Young's Double Slit experiment in optics, but applied to the superconducting macroscopic wavefunction.

In a SQUID, the superconducting loop is interrupted by one or two Josephson junctions. When a bias current is applied, it splits into two branches (or paths) around the loop. The quantum phase of the superconducting wavefunction evolves differently along each path depending on the local magnetic vector potential. When these paths recombine, the wavefunctions interfere either constructively or destructively.

This interference determines the maximum supercurrent the device can sustain (the critical current, I_c). Just as the intensity of light on a screen varies with the path difference in optics, the critical current of a SQUID varies periodically with the magnetic flux threading the loop.

9.2 Flux Sensitivity Mechanism

The fundamental sensitivity mechanism arises from the constraint of single-valuedness of the wavefunction. As derived in part 1, the total phase change around a closed superconducting loop must be an integer multiple of 2π.

In the presence of an external magnetic flux Φ_{ext}, the phase difference across the Josephson junctions (δ_1 and δ_2) is no longer independent. The phase constraint equation forces the sum of the phase drops across the junctions to equal the magnetic flux phase shift:

$$\delta_2 - \delta_1 = \frac{2\pi\Phi}{\Phi_0} \tag{12}$$

where Φ is the total flux in the loop (external flux + self-induced flux) and Φ_0 is the flux quantum.

This equation is the "heart" of the SQUID: it rigidly links a magnetic quantity (Φ) to a quantum mechanical variable (δ), which in turn controls the electrical transport (I_c).

10 TYPES OF SQUIDS

SQUIDs are categorized based on their biasing method (Direct Current vs. Radio Frequency) and the number of junctions employed.

10.1 DC SQUID

The Direct Current (DC) SQUID is the most sensitive and widely used architecture today.

- **Structure:** It consists of a superconducting ring interrupted by **two** Josephson junctions connected in parallel.
- **Operation:** The device is biased with a constant DC current I_b, typically slightly larger than the critical current of the two junctions ($I_b > 2I_c$).
- **Mechanism:** Because the bias current exceeds the critical current, the device operates in the resistive voltage state (according to the AC Josephson effect). However, the *magnitude* of this voltage depends on the critical current, which is modulating with the external magnetic flux.

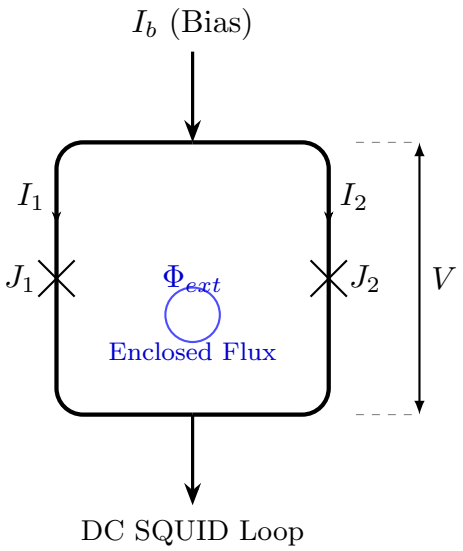

Figure 5: Circuit diagram of a DC SQUID. The device consists of two Josephson junctions (J_1, J_2) connected in parallel. The interference between the two paths makes the output voltage V extremely sensitive to the magnetic flux Φ threading the loop.

The DC SQUID effectively acts as a magnetic flux sensor with a bandwidth from DC up to several GHz.

10.2 RF SQUID

The Radio Frequency (RF) SQUID was historically significant due to simpler fabrication requirements (requir-

ing only one junction) but is less common in modern ultra-sensitive applications.

- **Structure:** It consists of a superconducting ring interrupted by a **single** Josephson junction.
- **Operation:** Since a single junction cannot be biased with a DC current to produce a voltage drop (the ring would just short out), it is inductively coupled to an external LC tank circuit driven at a radio frequency (typically 20–30 MHz).
- **Mechanism:** The SQUID loop acts as a variable impedance transformer. As the external magnetic flux changes, the effective inductance of the SQUID loop changes. This alters the resonant properties (quality factor Q and resonant frequency) of the tank circuit. By monitoring the voltage amplitude of the RF drive, one can deduce the flux in the SQUID loop.

11 I-V CHARACTERISTICS AND TRANSFER FUNCTION

To utilize the SQUID as a sensor, we must quantify how the electrical output (Voltage) relates to the magnetic input (Flux).

11.1 Critical Current Modulation

For a symmetric DC SQUID (where both junctions have identical critical currents I_0), the total critical current of the device $I_c(\Phi)$ modulates according to an interference pattern:

$$I_c(\Phi) = 2I_0 \left|\cos\left(\pi \frac{\Phi}{\Phi_0}\right)\right| \tag{13}$$

Physical Intuition:

- When $\Phi = n\Phi_0$ (integer flux quanta), the wavefunctions in both arms interfere constructively. The device can carry the maximum supercurrent $2I_0$ without resistance.
- When $\Phi = (n + \frac{1}{2})\Phi_0$ (half-integer flux quanta), the wavefunctions interfere destructively. The circulating current opposes the bias current in one arm, effectively reducing the net supercurrent capacity to zero (in the ideal case).

11.2 Voltage–Flux Characteristics

In practical operation, we bias the SQUID with a constant current I_b that is greater than the maximum critical current ($I_b > 2I_0$). The voltage across the SQUID is roughly determined by the "excess" current that cannot be carried as supercurrent and must flow as normal (resistive) current.

- If $I_c(\Phi)$ is high (constructive interference), more current travels as supercurrent, so the resistive voltage drop is *low*.
- If $I_c(\Phi)$ is low (destructive interference), less current travels as supercurrent, forcing more through the resistance, making the voltage drop *high*.

This results in a voltage $V(\Phi)$ that oscillates periodically with period Φ_0.

11.3 Flux-to-Voltage Transfer Function

The efficiency of the SQUID as a transducer is defined by its transfer function, denoted as V_Φ:

$$V_\Phi = \left|\frac{\partial V}{\partial \Phi}\right| \tag{14}$$

This parameter represents the slope of the V-Φ curve.

- The sensitivity is maximized where the slope is steepest (typically at $\Phi \approx (n \pm \frac{1}{4})\Phi_0$).
- In typical devices, this transfer coefficient is on the order of $V_\Phi \approx 100\ \mu\text{V}/\Phi_0$.

Implication for Measurement: Because the response is periodic (non-linear), a SQUID cannot be used directly to measure large changes in magnetic field (e.g., distinguishing between 0 and $100\Phi_0$ is impossible from voltage alone). To solve this, SQUIDs are almost always operated in a **Flux Locked Loop (FLL)**. This feedback circuit actively applies a magnetic field to cancel out any external changes, locking the SQUID at a fixed operating point (e.g., the steepest part of the slope). The current required to maintain this lock becomes the linear readout of the external field.

NOISE, SENSITIVITY, AND QUANTUM LIMITS

12 INTRODUCTION

The utility of a SQUID is defined not merely by its ability to transduce magnetic flux into voltage, but by its ability to resolve minute signals against a background of fluctuations. In this part, we analyze the stochastic processes that degrade signal integrity, starting from classical thermal noise and extending to the fundamental Heisenberg uncertainty principle. Understanding these limits is essential for designing ultra-sensitive magnetometers and quantum information processors.

13 NOISE SOURCES IN SQUIDS

Noise in SQUIDs arises from both intrinsic mechanisms (fundamental to the device physics) and extrinsic sources (environmental coupling).

13.1 Thermal Noise (Johnson-Nyquist Noise)

At any non-zero temperature T, the shunt resistors used to overdamp the Josephson junctions generate voltage fluctuations due to the thermal agitation of charge carriers. This is the dominant noise source in SQUIDs operating in the classical regime (typically 4.2 K).

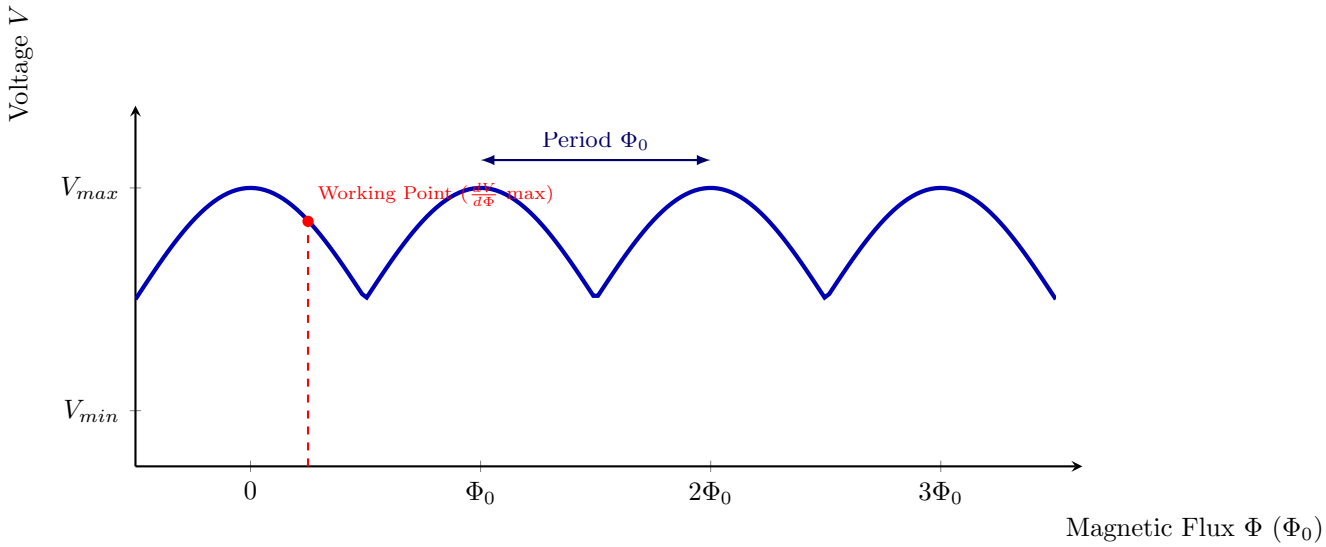

Figure 6: The Voltage-Flux (V-Φ) characteristic of a DC SQUID. The output voltage is a periodic function of the external flux with a period of one flux quantum Φ_0. For magnetometry, the SQUID is typically biased at the steepest part of the curve to maximize sensitivity.

The spectral density of the voltage noise S_V across the shunt resistance R is given by the Nyquist formula:

$$S_V(f) = 4k_BTR \tag{15}$$

where k_B is the Boltzmann constant. This voltage noise translates into an equivalent flux noise S_Φ via the transfer function $V_\Phi = |\partial V/\partial \Phi|$ derived in Part III:

$$S_\Phi(f) = \frac{S_V(f)}{V_\Phi^2} \approx \frac{4k_BTR}{V_\Phi^2} \tag{16}$$

To minimize this noise, one must maximize V_Φ or reduce the operating temperature T. This explains the drive towards milli-Kelvin operation for quantum computing applications.

13.2 Flux Noise

Flux noise refers to fluctuations that appear directly as magnetic flux in the SQUID loop, rather than voltage noise in the readout electronics.

This noise often originates from the motion of trapped vortices in the superconducting film or fluctuations in the currents of the input coil. In High-T_c SQUIDs, thermal hopping of vortices between pinning sites is a significant source of flux noise, often necessitating complex fabrication techniques to create "clean" films.

13.3 1/f Noise (Flicker Noise)

At low frequencies (typically below 1 Hz to 1 kHz), the noise spectral density increases inversely with frequency:

$$S_\Phi(f) \propto \frac{1}{f^\alpha}, \quad \alpha \approx 1 \tag{17}$$

The microscopic origin of $1/f$ noise in SQUIDs is a subject of ongoing research but is generally attributed to:

- **Critical Current Fluctuations:** Trapping and detrapping of charges in defects within the Josephson junction barrier, which modulates I_c.
- **Magnetic Spin Fluctuations:** Reorientation of surface spins on the superconducting material or the substrate.

Techniques such as *bias reversal* (chopping the bias current) are often employed to modulate the signal to a higher frequency, effectively bypassing the $1/f$ noise regime.

14 SENSITIVITY AND RESOLUTION

Sensitivity quantifies the smallest signal a SQUID can detect, usually defined where the signal-to-noise ratio (SNR) is unity.

14.1 Magnetic Field Sensitivity

While the SQUID detects magnetic flux Φ, practical applications often require measuring the magnetic field B. The relationship depends on the effective pickup area A_{eff}:

$$B = \frac{\Phi}{A_{eff}} \tag{18}$$

However, simply increasing the loop size to increase A_{eff} increases the loop inductance L, which degrades the transfer function V_Φ and increases noise.

To solve this, SQUIDs use a **flux transformer**: a large, external pickup loop (with large area A_p and inductance L_p) connected to a multi-turn input coil (inductance L_i) tightly coupled to the SQUID washer. This impedance matching allows SQUIDs to achieve field sensitivities on the order of $1 - 10$ fT/$\sqrt{\text{Hz}}$ (femtotesla per root Hertz), sufficient to detect neuro-

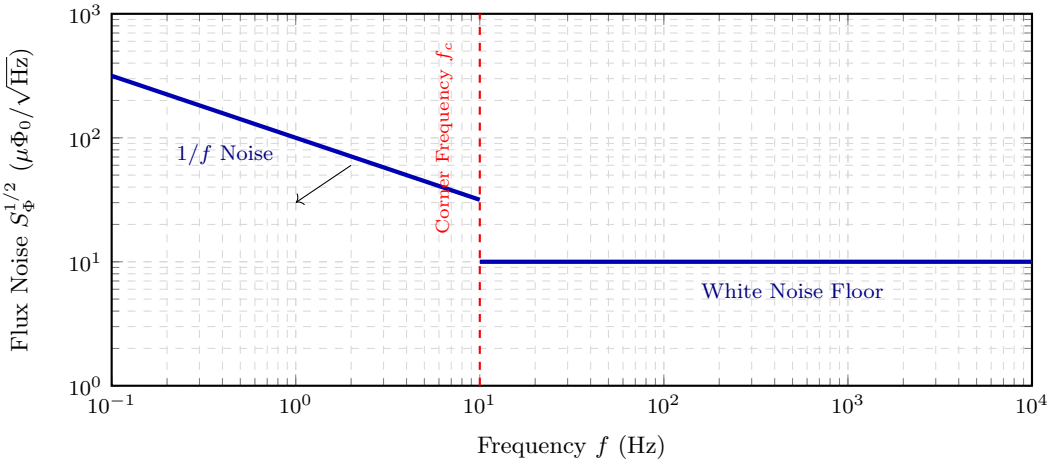

Figure 7: Noise power spectral density of a typical DC SQUID. The spectrum highlights the $1/f$ regime at low frequencies and the intrinsic white noise floor ($S_\Phi \approx 10^{-6}\Phi_0/\sqrt{\text{Hz}}$) at higher frequencies, with the transition occurring at the corner frequency f_c.

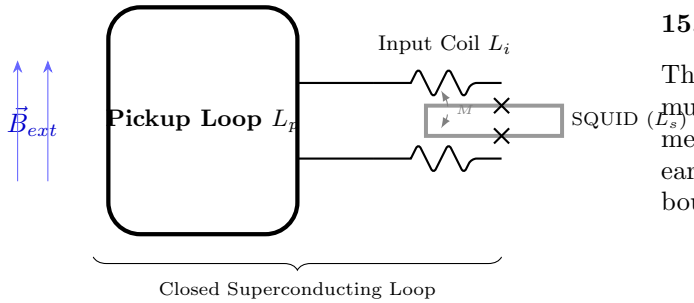

Figure 8: Schematic of a superconducting flux transformer. The external magnetic field induces a persistent current in the large pickup loop L_p, which is then converted into a local magnetic flux at the SQUID via the input coil L_i through mutual inductance M.

magnetic signals from the human brain (magnetoencephalography).

14.2 Energy Resolution

A more fundamental figure of merit is the energy resolution per unit bandwidth, ϵ. This metric accounts for the trade-off between inductance L and flux noise S_Φ:

$$\epsilon = \frac{S_\Phi}{2L} \tag{19}$$

In the thermal noise limit, optimizing the SQUID parameters yields:

$$\epsilon \approx 16 k_B T \sqrt{LC} \tag{20}$$

For a typical DC SQUID at 4.2 K, ϵ is on the order of 10^{-32} to 10^{-30} J/Hz, approaching the scale of Planck's constant h.

15 QUANTUM NOISE AND LIMITS

As operating temperatures are lowered and devices are miniaturized, thermal noise is suppressed until the zero-point fluctuations of the vacuum become the dominant noise source.

15.1 Standard Quantum Limit (SQL)

The Standard Quantum Limit represents the minimum measurement uncertainty imposed by quantum mechanics on a continuous measurement. For a linear amplifier like a SQUID, the energy resolution is bounded by the uncertainty principle:

$$\epsilon \geq \frac{\hbar}{2} \tag{21}$$

This limit arises because the SQUID is not a passive observer; the measurement process itself perturbs the system.

15.2 Backaction and Measurement Disturbance

The coupling between the SQUID and the system being measured is bidirectional.

- **Forward Action:** The system's flux affects the SQUID's circulating current.
- **Backaction:** The fluctuating circulating current in the SQUID loop generates a noisy magnetic field that couples back into the system.

According to the uncertainty principle, reducing the uncertainty in the measurement of flux ($\Delta\Phi$) inevitably increases the uncertainty in the conjugate variable, which is the charge (or voltage) across the capacitor, leading to increased backaction noise. The SQL is the point where the noise from the readout (imprecision) and the noise induced by the readout (backaction) are balanced and minimized.

15.3 Quantum-Limited Amplification

Recent advancements in Superconducting Parametric Amplifiers (transporting SQUID concepts into microwave cavities) have allowed researchers to approach and even bypass the standard limits.

Squeezed States: It is possible to circumvent the SQL by "squeezing" the uncertainty. If we allow the noise in one quadrature (e.g., amplitude) to increase, we can reduce the noise in the conjugate quadrature (e.g., phase) below the vacuum limit. This technique is now central to reading out superconducting qubits with high fidelity, marking the transition of SQUIDs from sensitive classical magnetometers to essential components of quantum computers.

FABRICATION AND MATERIALS SCIENCE

16 INTRODUCTION

The theoretical elegance of SQUIDs relies entirely on the quality of their physical realization. The performance of a SQUID—its critical current stability, noise floor, and hysteresis—is dictated by the materials chosen and the precision of the microfabrication process. This part explores the transition from theoretical models to physical devices, covering the two dominant material classes (Low-T_c and High-T_c) and the complex lithographic processes required to engineer quantum junctions.

17 SUPERCONDUCTING MATERIALS

The choice of superconducting material determines the operating temperature (T_{op}), the coherence length (ξ), and the fabrication complexity.

17.1 Nb-based SQUIDs (Low-T_c)

Niobium (Nb) is the industry standard for ultrasensitive SQUIDs and superconducting quantum computing qubits.

- **Properties:** Nb is an elemental Type II superconductor with a critical temperature $T_c \approx 9.2$ K. It is mechanically rugged, chemically stable against atmospheric oxidation (forming a protective Nb_2O_5 layer), and has a relatively long coherence length ($\xi \approx 38$ nm).
- **Junction Technology:** The standard junction is the Nb/Al-AlO_x/Nb trilayer. Aluminum is deposited on the base Nb layer and oxidized to form a pristine, pinhole-free insulating barrier (AlO_x) before the counter-electrode Nb is deposited.
- **Advantages:** This material system yields highly reproducible, non-hysteretic junctions with low $1/f$ noise. Because the coherence length is large, the fabrication tolerances are manageable (micrometer scale).

17.2 High-T_c SQUIDs (YBCO)

Yttrium Barium Copper Oxide ($YBa_2Cu_3O_{7-\delta}$, or YBCO) allows for operation at liquid nitrogen temperatures (77 K).

- **Properties:** YBCO is a complex ceramic oxide with $T_c \approx 92$ K. It is highly anisotropic; superconductivity occurs primarily within the copper-oxide planes (*ab*-planes). The coherence length is extremely short ($\xi_{ab} \approx 2$ nm, $\xi_c \approx 0.2$ nm).
- **Challenges:** The short coherence length means that even atomic-scale defects at the grain boundaries can disrupt the supercurrent. Unlike Nb, one cannot simply oxidize YBCO to make a barrier.
- **Junction Technology:** Instead of trilayers, High-T_c SQUIDs use *grain boundary junctions*. These are formed by growing the YBCO film on a bicrystal substrate (e.g., $SrTiO_3$) with a specific misorientation angle (typically 24°). The resulting dislocation network at the interface acts as the weak link.

18 MICROFABRICATION TECHNIQUES

Fabricating a SQUID requires creating a macroscopic loop interrupted by microscopic junctions. This is achieved through multi-stage photolithography.

18.1 Thin Film Deposition

The foundation of the device is the deposition of high-quality superconducting films.

- **DC Magnetron Sputtering:** The standard method for Niobium. Argon ions bombard a pure Nb target, ejecting atoms that condense onto the substrate (typically Silicon or Sapphire). This produces dense, polycrystalline films.
- **Pulsed Laser Deposition (PLD):** The preferred method for YBCO. A high-power excimer laser ablates a stoichiometric YBCO target. The plume of plasma condenses on a heated substrate ($700 - 800$°C) in an oxygen environment to ensure correct crystal growth and oxygen content.

18.2 Lithography

Patterning the geometry of the SQUID washer and input coils involves photolithography.

1. **Resist Application:** A photosensitive polymer (photoresist) is spin-coated onto the wafer.
2. **Exposure:** UV light is projected through a chrome-on-glass mask, transferring the circuit pattern to the resist.
3. **Development:** The soluble parts of the resist are washed away, leaving a protective mask over the areas where the superconductor should remain.

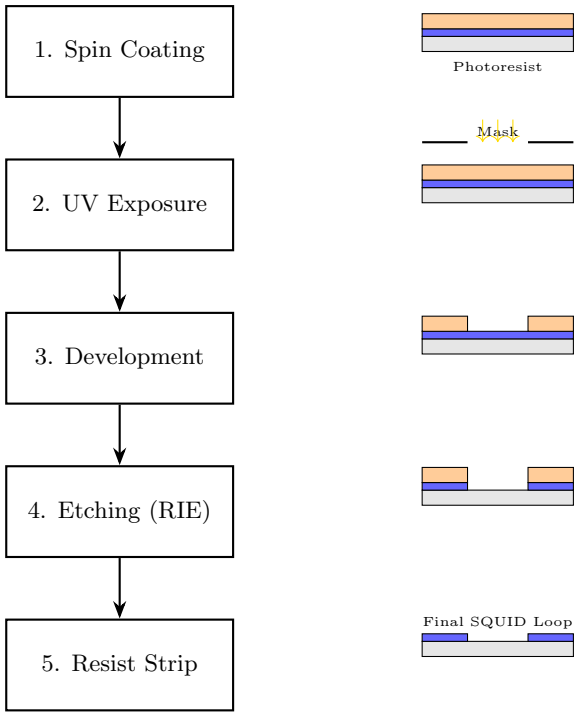

Figure 9: Process flow for SQUID fabrication: From a uniform Niobium film to the final patterned geometry via UV lithography and Reactive Ion Etching (RIE).

18.3 Junction Patterning (The Trilayer Process)

Defining the Josephson junction area is the most critical step. For Nb/Al-AlO_x/Nb devices, the "SNAP" (Selective Niobium Anodization Process) or "SNEP" (Selective Niobium Etch Process) is used.

- **Definition:** After depositing the full trilayer, a reactive ion etch (RIE) using gases like CF_4 or SF_6 removes the counter-electrode everywhere except at the junction site.
- **Anodization:** The exposed edges of the junction are anodized (converted to oxide) to insulate the base electrode from the subsequent wiring layer.
- **Wiring:** A final wiring layer of Nb is deposited to connect the top of the junction to the rest of the circuit.

19 CRYOGENIC INTEGRATION

SQUIDs must be cooled well below their T_c to operate. The cryogenic infrastructure is an integral part of the sensing system.

19.1 Dilution Refrigerators

For ultra-low noise applications (e.g., quantum computing or gravity wave detection), 4.2 K (Liquid Helium) is insufficient due to thermal noise. Dilution refrigerators are used to reach milli-Kelvin temperatures ($10 - 20$ mK).

- **Principle:** The cooling power is derived from the heat of mixing as ^{3}He atoms cross the phase boundary from a ^{3}He-rich phase to a ^{3}He-poor phase (dissolved in ^{4}He). This is an endothermic process that works even at absolute zero limits, unlike evaporative cooling.

19.2 Magnetic Shielding

Because SQUIDs are sensitive to femtotesla fields, environmental noise (Earth's field ≈ 50 µT, power line hum, moving elevators) must be attenuated by factors of 10^6 to 10^8.

- **Mu-Metal Shields:** High-permeability nickel alloys ($\mu_r \approx 100,000$) divert magnetic flux lines around the sample chamber.
- **Superconducting Shields:** A superconducting can (e.g., Lead or Niobium) cooled below T_c expels all external flux via the Meissner effect, creating a theoretically field-free region for the SQUID.

19.3 Readout Electronics (Flux Locked Loop)

As established in part 3, the voltage response of a SQUID is non-linear (sinusoidal). To linearize the output and increase dynamic range, the **Flux Locked Loop (FLL)** is used.

1. **Measurement:** The SQUID voltage is amplified and fed into an integrator.
2. **Feedback:** The integrator output drives a current through a feedback coil inductively coupled to the SQUID.
3. **Nulling:** This feedback current generates a magnetic flux exactly equal and opposite to the external flux change.
4. **Output:** The voltage across the feedback resistor is linearly proportional to the external flux.

SQUIDS IN QUANTUM TECHNOLOGIES

20 INTRODUCTION

In the previous parts, we treated the SQUID primarily as a sensor—a device that measures classical signals (magnetic flux) with quantum sensitivity. In this part, we explore the SQUID as a quantum object in its own right. By exploiting the non-linear inductance of the Josephson junction and the macroscopic quantum coherence of the superconducting loop, SQUIDs form the basis of Superconducting Qubits—the leading platform for building scalable quantum computers. Furthermore, SQUID-based amplifiers enable the readout of these quantum states with fidelity approaching the fundamental limits of nature.

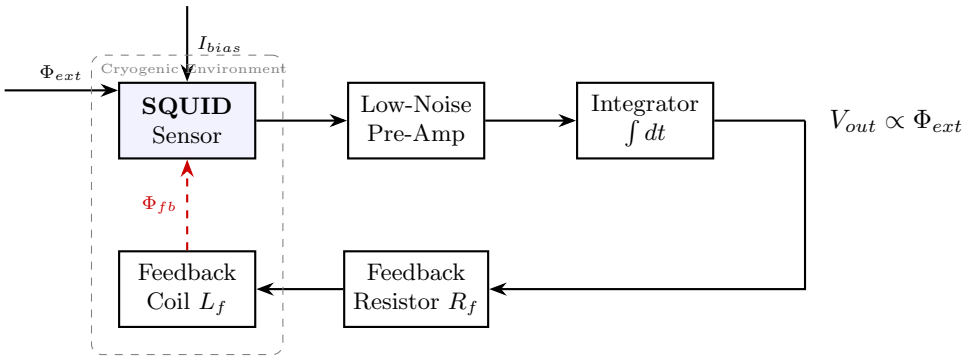

Figure 10: Block diagram of the Flux Locked Loop (FLL). The integrator output is converted into a feedback current that maintains the SQUID at a constant flux state, effectively "locking" it to a specific point on the V-Φ curve.

21 SQUIDS AS QUBITS

To create a qubit (quantum bit), one requires a quantum system with two distinct energy levels ($|0\rangle$ and $|1\rangle$) that can be manipulated coherently. A simple LC harmonic oscillator (like a superconducting tank circuit) has equally spaced energy levels ($E_n = \hbar\omega(n + 1/2)$), making it impossible to isolate the $|0\rangle \to |1\rangle$ transition without exciting $|1\rangle \to |2\rangle$.

The Josephson junction acts as a non-linear inductor, introducing anharmonicity into the potential well. This creates unequal spacing between energy levels, allowing the ground and excited states to be uniquely addressed with microwave pulses.

21.1 Flux Qubits

The Flux Qubit is topologically a superconducting loop interrupted by three Josephson junctions.

- **Potential Landscape:** When the external magnetic flux threading the loop is near $\Phi_0/2$, the potential energy of the system forms a "double-well" potential.
- **Quantum States:** The two wells correspond to macroscopic persistent currents circulating in opposite directions (clockwise $|\circlearrowright\rangle$ and counter-clockwise $|\circlearrowleft\rangle$).
- **Superposition:** At the degeneracy point, the eigenstate is a quantum superposition of these two macroscopic currents:

$$|\psi\rangle = \frac{1}{\sqrt{2}}(|\circlearrowright\rangle + |\circlearrowleft\rangle) \tag{22}$$

This was one of the first demonstrations of macroscopic quantum coherence, where billions of Cooper pairs simultaneously flow in two directions at once.

21.2 Phase Qubits

The Phase Qubit utilizes a single current-biased Josephson junction.

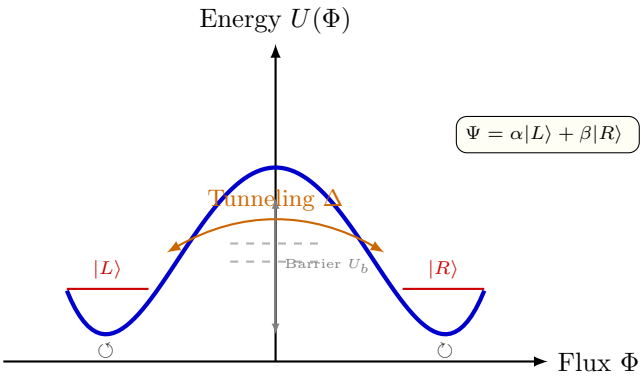

Figure 11: The double-well potential of a superconducting flux qubit. At the degeneracy point, the system can tunnel between the two persistent current states. The energy splitting at the center represents the qubit's gap Δ, which prevents the states from being exactly degenerate due to quantum fluctuations.

- **Potential Landscape:** The potential is the "tilted washboard" potential derived from the Josephson energy:

$$U(\delta) = -E_J \cos\delta - I_b \frac{\Phi_0}{2\pi}\delta \tag{23}$$

where δ is the phase difference and I_b is the bias current.

- **Operation:** By biasing the junction close to the critical current I_c, the potential wells become shallow and support only a few quantized energy levels.
- **Drawback:** Phase qubits have short coherence times (T_1, T_2) due to their sensitivity to charge noise and bias fluctuations, leading to their eventual replacement by Transmons.

21.3 Transmon Evolution

The Transmission Line Shunted Plasma Oscillation Qubit (Transmon) is currently the most widely used superconducting qubit (e.g., in IBM and Google processors).

- **Structure:** It is essentially a Cooper Pair Box (a small superconducting island) shunted by a very large capacitor.
- **Role of the SQUID:** The inductive element of a Transmon is often a DC SQUID loop rather than a single junction. This allows the transition frequency of the qubit (ω_q) to be tuned by applying an external magnetic flux to the SQUID loop.
- **Physics:** The large capacitance (C_S) lowers the charging energy E_C, making the energy levels insensitive to charge noise (fluctuations in the DC electric environment). The SQUID provides the necessary Josephson energy E_J to maintain anharmonicity.
- **Result:** Coherence times have improved from nanoseconds (in early Cooper Pair Boxes) to hundreds of microseconds in modern Transmons.

22 QUANTUM MEASUREMENT AND READOUT

Reading out the state of a superconducting qubit requires detecting a single microwave photon's worth of energy—a task that pushes SQUID technology to the quantum limit.

22.1 Dispersive Readout

Modern readout does not measure the qubit directly (which would destroy the state via relaxation). Instead, it uses Circuit Quantum Electrodynamics (cQED).

- **Setup:** The qubit is capacitively coupled to a superconducting microwave resonator (cavity).
- **Interaction:** In the dispersive regime (where the qubit frequency ω_q is far detuned from the cavity frequency ω_r), the interaction leads to a state-dependent frequency shift of the cavity:

$$\omega_r' = \omega_r \pm \chi \tag{24}$$

  where the sign depends on whether the qubit is in $|0\rangle$ or $|1\rangle$.
- **Measurement:** By reflecting a microwave pulse off the cavity and measuring its phase shift, one can deduce the qubit state without absorbing energy from the qubit itself.

22.2 Parametric Amplifiers (JPA/TWPA)

The signal exiting the readout cavity is extremely weak (approx. -140 dBm). Conventional semiconductor amplifiers (HEMTs) add too much thermal noise.

- **Concept:** A Josephson Parametric Amplifier (JPA) uses a SQUID or a series of SQUIDs as a non-linear medium.
- **Operation:** A strong "pump" tone is applied at twice the signal frequency (2ω) or a nearby frequency. The non-linear inductance of the SQUID mixes the pump and signal, transferring energy from the pump to the signal.
- **Noise Performance:** JPAs can amplify signals with added noise at the quantum limit ($T_{noise} \approx \hbar\omega/k_B$), which is essential for high-fidelity single-shot readout.

22.3 Quantum Non-Demolition (QND) Measurement

A QND measurement allows one to determine the eigenvalue of an observable (like the qubit energy state) without changing the eigenstate itself.

- Because the Dispersive Readout measures the *frequency shift* of the cavity rather than absorbing a photon from the qubit, the qubit remains in its $|0\rangle$ or $|1\rangle$ state after measurement.
- This capability is crucial for Quantum Error Correction, where one must measure "syndrome" qubits to detect errors without destroying the quantum information encoded in the "data" qubits.

23 HYBRID QUANTUM SYSTEMS

SQUIDs act as the perfect interface between different quantum degrees of freedom (spins, photons, phonons) due to their extreme sensitivity and wide bandwidth.

23.1 Coupling to Microwave Cavities

As discussed in Section 6.2.1, SQUIDs couple naturally to microwave photons. This "Circuit QED" architecture allows:

- **Long-range coupling:** Two qubits separated by centimeters can interact via a virtual photon in a shared bus resonator.
- **Quantum Memory:** Qubit states can be swapped into high-Q cavities (photonic states) for longer storage times.

23.2 Spin–SQUID Interfaces

Electron spins (like Nitrogen-Vacancy centers in diamond or Phosphorus donors in Silicon) have excellent coherence times but are hard to couple to each other.

- **Mechanism:** A SQUID can detect the magnetic dipole field of a spin ensemble. By placing the spins in the near-field of a flux-tunable resonator (SQUID), one can achieve strong coupling.
- **Application:** This enables the conversion of quantum information from the optical domain (NV centers) to the microwave domain (superconducting processors).

23.3 Mechanical Resonator Coupling

SQUIDs are also used to probe the quantum limits of motion in macroscopic objects.

- **Setup:** A nanomechanical beam is coated with a superconductor or coupled to a SQUID loop.
- **Interaction:** The motion of the beam changes the inductance or flux in the circuit.
- **Goal:** This field, known as *Circuit Optomechanics*, allows researchers to cool massive objects to their motional ground state and create "Schrödinger's Cat" states of mechanical motion, testing the validity of quantum mechanics at macroscopic scales.

ADVANCED TOPICS AND RESEARCH FRONTIERS

24 INTRODUCTION

Having established the SQUID as both a premier sensor and a qubit, this final part addresses the frontiers of the field. Current research pushes SQUIDs beyond the Standard Quantum Limit (SQL) using quantum optics techniques, modifies the fundamental Josephson relation using topological materials to create fault-tolerant qubits, and utilizes these devices to hunt for dark matter.

25 ULTRA-LOW NOISE AND QUANTUM METROLOGY

The sensitivity of a classical SQUID is limited by the Heisenberg Uncertainty Principle applied to the measurement process itself. To surpass this, we must manipulate the quantum state of the electromagnetic field entering the amplifier.

25.1 Squeezed States in SQUID Amplifiers

In a standard measurement, the vacuum fluctuations of the electromagnetic field impose a noise floor equivalent to $\frac{1}{2}\hbar\omega$ (zero-point energy). These fluctuations are distributed equally between the two quadrature components of the field, $\hat{X}_1$ (amplitude-like) and $\hat{X}_2$ (phase-like), such that $\Delta X_1 \Delta X_2 \geq 1/4$.

A **Josephson Parametric Amplifier (JPA)** can be operated in a "phase-sensitive" mode to generate squeezed states.

- **Mechanism:** By modulating the inductance of the SQUID at twice the signal frequency ($2\omega_s$), the JPA amplifies one quadrature ($\hat{X}_1$) while attenuating the conjugate quadrature ($\hat{X}_2$).
- **Result:** The noise in the attenuated quadrature is reduced *below* the vacuum level ($\Delta X_2^2 < 1/4$), at the cost of increased noise in the amplified quadrature.
- **Application:** If the signal of interest is encoded entirely in the "quiet" quadrature, the Signal-to-Noise Ratio (SNR) can exceed the limit imposed by the vacuum fluctuations of a standard linear amplifier.

25.2 Heisenberg-Limited Detection

The Standard Quantum Limit (SQL) for estimating a parameter (like magnetic flux Φ) scales as $1/\sqrt{N}$, where N is the number of photons (or measurement resources). Quantum metrology aims for the **Heisenberg Limit**, which scales as $1/N$.

Achieving this requires using entangled probe states, such as N00N states ($|\psi\rangle = \frac{1}{\sqrt{2}}(|N,0\rangle + |0,N\rangle)$), inside the SQUID loop. While generating large-N entangled states is challenging, injecting squeezed vacuum into the input port of a SQUID interferometer has been experimentally demonstrated to improve sensitivity by several decibels over the shot-noise limit, crucial for detecting ultra-weak signals like gravitational waves or axions.

26 TOPOLOGICAL AND EXOTIC JOSEPHSON DEVICES

Standard Josephson junctions tunnel Cooper pairs ($2e$ charge) between s-wave superconductors. Replacing the standard barrier with a topological material fundamentally alters the current-phase relation.

26.1 Majorana-based SQUIDs

Topological Superconductors are predicted to host **Majorana Zero Modes (MZMs)** at their boundaries. These are non-Abelian quasiparticles that are their own antiparticles ($\gamma^\dagger = \gamma$).

- **Setup:** A "Majorana SQUID" consists of a topological nanowire (e.g., InAs with strong spin-orbit coupling, proximity-coupled to a superconductor) interrupted by a weak link, forming a loop.
- **Physics:** The MZMs residing at the junction interface allow for the coherent tunneling of single electrons, rather than pairs, without breaking Cooper pairs in the bulk.
- **Significance:** MZMs are topologically protected; local noise cannot decohere the quantum information stored in them. This is the basis for *Topological Quantum Computing*.

26.2 4π-Periodic Josephson Effect

The hallmark signature of Majorana-mediated tunneling is a change in the periodicity of the Josephson energy-phase relation.

- **Standard Junction:** $E(\phi) \propto \cos(\phi)$. The system returns to its ground state after the phase winds by 2π.

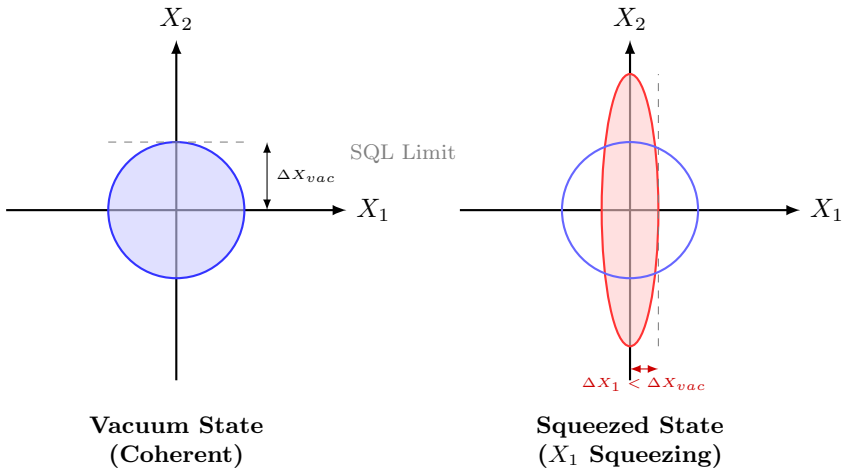

Figure 12: Phase space representation (Wigner distribution) showing the standard quantum limit of a vacuum state versus a squeezed state. SQUID-based Josephson Parametric Amplifiers (JPAs) are used to generate these states to improve the signal-to-noise ratio in qubit readout.

- **Topological Junction:** The tunneling of a single electron (charge e) implies the phase must wind by 4π to restore the system to its original state.

$$I_s \propto \sin(\phi/2) \tag{25}$$

- **Observation:** In an AC Josephson experiment, this manifests as the absence of odd-numbered Shapiro steps. Under microwave irradiation, voltage steps normally appear at $V_n = n\frac{hf}{2e}$. For a 4π-periodic junction, steps only appear at even integers ($n = 2, 4, \dots$), effectively doubling the voltage step height.

27 FUTURE DIRECTIONS

Research in SQUIDs is bifurcating into two main streams: massive scaling for computing and extreme sensitivity for fundamental physics.

27.1 Scalable Quantum Circuits

As superconducting processors scale past 1000 qubits, the "wiring bottleneck" becomes critical.

- **3D Integration:** Future SQUID arrays will likely utilize Flip-Chip technology, where the qubit chip is bump-bonded to a separate readout/wiring interposer chip.
- **TSVs (Through-Silicon Vias):** Superconducting vias allow signals to pass vertically through the silicon substrate, enabling dense 2D arrays of SQUIDs without wire clutter on the surface.
- **Cryogenic CMOS:** Integrating classical control electronics (Cold CMOS) directly at 4 K to control the SQUID arrays at 10 mK, reducing the number of coaxial cables running to room temperature.

27.2 Quantum Sensors for Dark Matter

SQUIDs are the primary detector for Axions, a leading Dark Matter candidate.

- **The Haloscope:** The ADMX (Axion Dark Matter Experiment) uses a high-Q microwave cavity in a strong magnetic field. An axion converting into a photon would produce a microwave signal at a frequency corresponding to the axion mass.
- **Signal Power:** The expected power is incredibly low ($\sim 10^{-24}$ Watts).
- **Role of SQUID:** A Microstrip SQUID Amplifier (MSA) or a JPA is coupled to the cavity to detect this excess power. Squeezed state injection (discussed in 7.1.1) is currently being implemented to scan through axion mass ranges faster than otherwise possible.

27.3 Integration with Quantum Processors

The ultimate vision is a "Quantum Internet" or distributed quantum computer.

- **Optical Transduction:** Superconducting qubits (microwave) cannot be transmitted over optical fibers (telecom wavelength). Electro-optic mechanical converters are being developed where a SQUID-modulated membrane converts microwave photons to optical photons.
- **Hybrid Logic:** Using ultra-fast SFQ (Single Flux Quantum) digital logic—which uses propagating flux pulses in SQUIDs—as a low-latency control layer for the quantum processor, replacing room-temperature AWGs (Arbitrary Waveform Generators).

28 CONCLUDING REMARKS

The SQUID has evolved from a laboratory curiosity verifying macroscopic quantum mechanics into a cor-

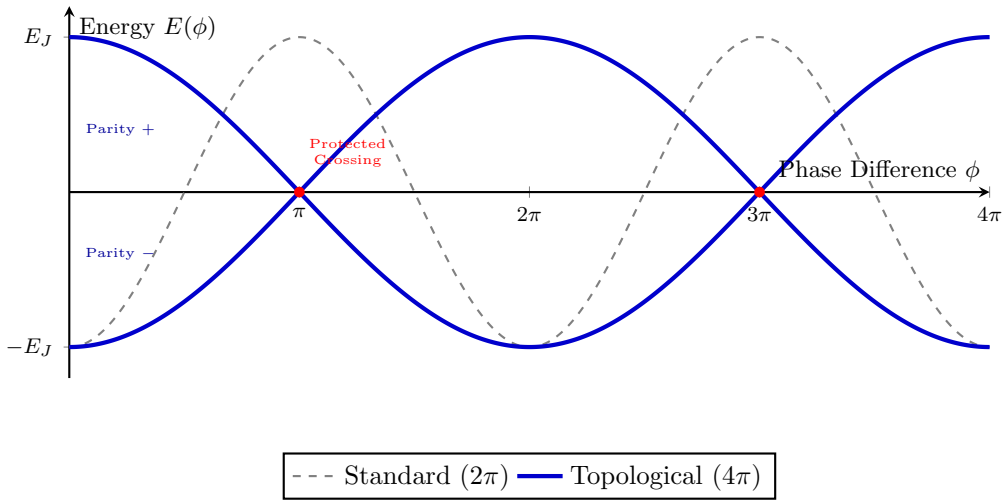

Figure 13: The energy-phase relation comparing a standard Josephson junction (dashed gray) and a topological junction (solid blue). The 4π periodicity arises from the fusion of Majorana fermions, where the system remains in a specific parity branch unless a quasiparticle poisoning event occurs.

nerstone of modern physics. Whether detecting the faintest magnetic fields of the brain, searching for the invisible matter of the universe, or processing information in a quantum computer, the Superconducting Quantum Interference Device remains the bridge between the quantum and classical worlds.

29 REFERENCES

29.1 Foundational Texts and Reviews

References

[1] Barone, A., & Paternò, G. (1982). *Physics and Applications of the Josephson Effect*. Wiley. (The primary text for junction physics).

[2] Clarke, J., & Braginski, A. I. (Eds.). (2004). *The SQUID Handbook: Vol. 1 Fundamentals and Technology of SQUIDs and SQUID Systems*. Wiley-VCH. (The most comprehensive technical manual in existence).

[3] Jenks, W. G., Sadeghi, S. S. H., & Wikswo, J. P. (1997). SQUIDs for nondestructive evaluation. *Journal of Physics D: Applied Physics*, **30**(3), 293–323. doi:10.1088/0022-3727/30/3/002.

[4] Kleiner, R., Koelle, D., Ludwig, F., & Clarke, J. (2004). Superconducting quantum interference devices: State of the art and applications. *Proceedings of the IEEE*, **92**(10), 1534–1548. doi:10.1109/JPROC.2004.833655.

29.2 Seminal Discoveries

References

[1] Bardeen, J., Cooper, L. N., & Schrieffer, J. R. (1957). Theory of superconductivity. *Physical Review*, **108**(5), 1175–1204. (The BCS Theory).

[2] Jaklevic, R. C., Lambe, J., Silver, A. H., & Mercereau, J. E. (1964). Quantum Interference Effects in Josephson Tunneling. *Physical Review Letters*, **12**(7), 159–160. (The first experimental demonstration of a SQUID).

[3] Josephson, B. D. (1962). Possible new effects in superconductive tunnelling. *Physics Letters*, **1**(7), 251–253. (The theoretical prediction of the Josephson effect).

29.3 Quantum Technology and Frontiers (2019–2026)

References

[1] Esposito, M., et al. (2019). Development and characterization of a flux-pumped lumped element Josephson parametric amplifier. *EPJ Web of Conferences*, **198**, 00008. doi:10.1051/epjconf/201919800008.

[2] Vettoliere, A., et al. (2019). Fine-tuning and optimization of superconducting quantum magnetic sensors by thermal annealing. *Sensors*, **19**(17), 3635. doi:10.3390/s19173635.

[3] Willsch, D., et al. (2024). Observation of Josephson harmonics in tunnel junctions. *Nature Physics*.

[4] Zhang, X., et al. (2025). Novel light dark matter detection with quantum parity detector using qubit arrays. arXiv preprint arXiv:2512.20309. (Cutting-edge application in dark matter searches).